Journal of
Entomology

CrossMark

Research Article
Morphogenesis of Early Embryonic Development in the Greater Wax Moth, *Galleria mellonella* (Lepidoptera: Pyralidae)

Muhamad Abidalla

Department of Sciences, University of Basilicata, Viale dell'Ateneo Lucano 10, 85100 Potenza, Italy

Abstract

Background and Objective: *Galleria mellonella* (*G. mellonella*) is an apicultural pest. The early embryonic development in *Galleria mellonella* is the target of this study, which is important in many subfields, including developmental biology, ecology and applied entomology. **Material and Methods:** By microscopy of whole mount preparations, the embryos samples were dechorionated, permeabilized and fixed before staining with different dyes. **Results:** The study provides a first timeline of morphological hallmarks during the following early developmental stages: (1) Maturation, fertilization and cleavage [0-4.5 h post-oviposition (PO)], (2) Blastoderm formation (5-11 h PO), (3) Germ disk, serosa formation and beginning of Amnion (12-22.5 h. PO) and (4) Immersion of germ disk into the yolk and formation of the germ band during anatrepsis movement (22-31 h PO). **Conclusion:** The whole mount method could be an easy way than the sectioning methods to study the embryogenesis of insect and studying the morphological markers that have a phylogenetic relation in same family species.

INTRODUCTION

The moth superfamily Pyraloidea is a species-rich group among Lepidoptera and the greater wax moth or honeycomb moth, *Galleria mellonella* (Linnaeus), is one pyraloid species that has become important in many different lines of research. *Galleria mellonella* is a beehive parasite[1] and it is used as an alternative infection model for the study of entomopathogenic and entomophagous interactions as well as an infection model in medical studies[2-5]. *G. mellonella* also has been used in studies of host-pathogen interactions and invertebrate immune systems[6,7]. Moreover, because its life in beehives occurs under highly stable thermal conditions, *G. mellonella* is a suitable species for studies of temperature-mediated changes in insect physiology and endocrinology[8-10] and for cryopreservation programs[11].

Comparative embryological studies are demonstrated many differences in the mode of embryonic development in basal lepidopterans versus higher ditrysians[12]. Here, it is compared the early embryonic development of *G. mellonella* with that of other species of Lepidoptera. There is a level of individual variation in the development rate among *G. mellonella* eggs. Early embryogenesis in Lepidopterans has been extensively characterized in several moths and in 22 advanced ditrysian species such as *Bombyx mori* (Linnaeus), *Pieris rapae* (Linnaeus) and *Manduca sexta* (Linnaeus)[13,14]. Also, in Crambidae, early embryogenesis has been characterized for three species, *Chilo suppressalis* (Walker) (Asiatic rice borer)[15] *Ancylolomia japonica* Zeller (rice webworm)[16,17] and *Diatraea saccharalis* Fabricius (sugarcane borer)[18]. In the present study, the morphology of early embryogenesis was observed without using sectioned samples stained with antibodies or molecular genetics dyes to facilitate microscopy. The whole mount method to study development during early embryonic stages was used because of: (1) The difficulty of embedding eggs in paraffin or resin for sectioning, (2) The high thickness of the chorion in the Lepidopteran egg, which requires that different slide-preparation methods be used for observation of Lepidopteran embryos, compared to those used for dipteran embryos. The aim of this study was succeed to provide the first visualization of embryogenesis in *G. mellonella*, this information will be useful in phylogenetic studies and in selection of the proper embryonic stage for cryopreservation programs. The morphogenesis of embryonic process is a topic of great interest in many subfields, including biology, ecology and applied entomology.

MATERIAL AND METHODS

This study was part of a doctoral dissertation in University of Basilicata (2010, Potenza, Italy). The reared larvae and microscopic experiments of *G. mellonella* embryos were carried out as joint research with the Centre for Agrobiological and Pedological Research (CREA-Agricultural Research Council, Florence, Italy).

Egg/embryo collecting and staging: Eggs and embryos were obtained from female *G. mellonella* reared for 6 months at a temperature of $26\pm2°C$ and relative humidity of $70\pm10\%$. Eggs were collected on an oviposition paper placed on the top of a cage containing 100-150 adults with a sex ratio of about 1:1. The oviposition period of females was limited to 30 min. Egg batches were then placed in aerated cages (10×20 cm) and incubated in a humidified chamber with near-normal honey bee brood nest conditions: Darkness, temperature $30\pm0.5°C$ and relative humidity $85\pm2\%$. Time zero was taken at the time when fertilized eggs were placed in the chamber. Under these conditions, embryogenesis of *G. mellonella* required 6 days (144 h) until hatching. A total of 360 embryos were obtained for observation of the morphological process, with 10-15 embryos being visualized per each interval time of 3 h. During this interval, it could be seen approximately 40-50% of the embryos with the same embryonic characteristics.

Sample preparation

Dechorionation: The removal of the chorion layer of eggs was performed mechanically and by manipulation with a thin needle or, alternatively, chemically with 3% NaOCl (containing approximately 7% active chlorine at final concentration) for 4-5 min. Dechorionated eggs were then permeabilized by short (2 sec) exposure to isopropanol to remove the residual water, which would otherwise prevent the effect of heptane that was applied for 10-20 sec to remove the wax layer. The eggs were then washed with PBS to remove the residual heptane and fixated with Carnoy's fixative (methanol: chloroform: acetic acid 6:3:1) for 3-4 h.

Toluidine blue-rhodamine B staining: TB has been proven suitable for studies of morphogenesis and development of insect embryos[19-21]. Rhodamine B is widely used as an indicator dye for the permeability of dechorionated eggs[22-24]. The primary staining with TB solution (prepared as 1 g of TB dissolved in 100 mL of 70% ethanol, pH 2.0~2.5) was applied at two different exposure times depending on the complexity of actual embryonic structure at various stages. The exposure

time was 3-5 min for the zygote until germ disk formation and 15-20 min for germ disk from gastrulation until germ band formation. For visualization of the separated nuclei, a secondary staining with Rhodamine B (0.1% in DW) for 1 sec exposure time was performed, followed by serial dehydration steps in ethanol (35, 50, 70, 80 and 95%) for 2-3 min per each concentration. The specimen was then kept in 70% ethanol at 4°C for image recording, to a maximum of 2 days. Then the eggs were mounted on coverslips with Canada balsam glue. Dehydration in a graded series of ethanol after the staining procedure decreased metachromasia effects (in which TB color changes from blue to purplish red) but did not affect the blue color of stained mitotic nuclei. To observe the details of the eggs' contents after deposition, the dechorionated/permeabilized eggs were stained with 0.1% Rhodamine B for 4 min (exposure time increased with continued development) (Fig. 1). For confocal and fluorescence microscopy, Rhodamine B. was sequentially excited, first with a laser at 514 nm and then with a xenon lamp at 540-525 nm sequentially. TB is a basic metachromatic nuclear stain with blue color and is commonly used in histological studies[25].

Hematoxylin-eosin staining: After dechorionation, permeabilization, fixation as was done before with TB, samples were exposed to hematoxylin for 6 min, then washed in distilled water for 5 min. Samples were then decolorized in acid alcohol for 1-3 sec then rinsed in DW for 5 min. Finally, samples were stained with Eosin for 1-2 min, followed by serial dehydration and mounting for final observation. For confocal microscopy, eosin fluorescence was observed after laser excitation at 514 nm.

Calcofluor white staining: The CFW dye was used to see the development of chitin in membranes (amnion and serosa). Samples were dechorionated, per-meabilized and fixated as done before with TB and then exposed to CFW dye [5 mg mL^{-1} Fluorescent Brightener 28 (SIGMA-ALDRICH) diluted in DMSO (dimethyl sulfoxide) at pH 12 calibrated by 2N KOH, resulting in a light-yellow solution, kept in dark]. Samples were CFW-stained for three separate times: For 18 min, 4 h and overnight, in the dark (4°C)[26]. Finally, the sample was washed with PBS (6.2 pH) for 2-3 times, re-suspended in 20% glycerol and visualized using an excitation wavelength of 340-380 nm for fluorescence and DIC. For confocal microscopy, the emission of CFW was visualized with laser AFP (514 nm). Calcofluor white (CFW) is a non-specific dye which preferentially binds to chitin cellulose in cell walls and as such is also used to visualize plant cells. The CWF has broad excitation/emission spectra and can be used in combination with broadband filters and most UV or blue light sources[27]. The CFW is one compound from a group of agents known as fluorescent brighteners or whiteners[28,29]. It has already been used to visualize chitin in nematode eggs[30] and *Drosophila melanogaster* Meigenembryos[31]. It binds with a high affinity to structural polysaccharides, β-1,3 and β-1,4 polysaccharides (cellulose) and chitin[32]. This study, found that the short emission time of the CFW failed under fluorescence microscope but after a few min of exposure, it was effective in the observation of embryogenesis by Nomarski DIC microscope. A polarizing filter was always used during capturing images and Adobe Photoshop was used to adjust images for better identification of morphological markers, even sometimes changing the color of embryos. All chemicals were purchased from Sigma Chemical Co. (St. Louis, MO).

Microscopy
Scanning electron microscope (SEM): The exterior egg surface was investigated and analyzed by SEM. Eggs were fixed in 2.5% glutaraldehyde buffered with 0.1 M phosphate buffer, pH. 7.4[33]. After fixation, the eggs were rinsed in phosphate buffer, treated with 1% OsO$_4$ in phosphate buffer and then dehydrated stepwise in an ethyl alcohol series. The eggs were then placed on a critical point drying device (CPD 020, Leica Microsystems GmbH, Germany) for 1 h. After dehydration, the eggs were transferred to a desiccator at 45°C and stored for 24 h, then mounted on stubs with a small drop of silver nitrate glue and transferred again to a desiccator to dry the glue. Finally, the mounted specimens were coated with a thin layer of gold with a S150A Sputter Coater and examined and photographed in the microscope (Philips 515 SEM).

Differential interference contrast (DIC): Images were acquired using 20x 0.45 NA plan Fluor (ELWD, NIKON, JAPAN) and 40x 0.60 NA PL Fluor (LEITZ) objectives.

Fluorescence microscopy: CFW based fluorescence-microscopic images were recorded using a DIC microscope equipped with an INTENSILIGHT C-HGFI/C-HGFIE Fiber Illuminator (xenon arc lamp, NIKON, C-HGFI, JAPAN) in

combination with filters of the excitation wavelengths 340-380 nm, 465 space -495 nm and 540-525 nm.

Confocal laser scanning microscopy: This microscope was performed with an A1 R+system (ALSI system) (NIKON, JAPAN) equipped with an Argon Ion laser (457-514 nm) and a diode-pumped solid-state (DPSS) emitting at 561 nm. The emission at the range of 457 nm and 514 nm was captured by frame grabber software (NIS Elements, Nikon, Japan) and subsequently transferred to Photoshop (Adobe, JAPAN) for further processing. Confocal recordings were performed with TB, H and E and CFW dyes. Pairs of single images were superimposed for visualization of co-localization. All micrographs shown are sections from serial Z-stack images 1 μm apart.

RESULTS AND DISCUSSION

The general observations of main markers and time scale of embryonic development stages in *G. mellonella* was characterized in Table 1. The life cycle of *G. mellonella* at 30°C was described in Fig. 1.

External characteristics: *Galleria mellonella* eggs vary slightly in shape from spheroidal to ellipsoid, ovoid or obovoid, with a maximum×minimum diameter (mm) of 0.70±0.05×0.55±0.03 (n = 25). Early embryos (deposited during the first 3 h) have a larger surface and size in comparison with late stages. Aeropyles are sparsely distributed over the entire surface of the egg but there are

fewer of them located on the anterior surface than elsewhere. Each egg bears 150-200 aeropyles with each opening measuring 1.6±0.6 μm (n = 25) (Fig. 1) and surrounded by a narrow to rather broad collar. The chorion is soft, fragile and thin (3.5 μm) immediately post-ovipostion (Fig. 1). The anterior end of the egg shows the petal of the micropylar rosette (Fig. 1). Superficial features of *G. mellonella* eggs were found to be identical to the description of Barbier and Chauvin[34].

Internal structures: The internal structure of newly laid eggs of *G. mellonella* has been compared with similarity to that described previously in *D. saccharalis* (Crambidae). Freshly deposited eggs contain a homogeneous granular yolk mass and were protected externally by a mucous substance secreted by the female. Different zones within the egg were visualized by Rhodamine B dye. One of these is the periplasm (PR), which is a layer of cytoplasm immediately under the chorion and vitelline membrane. Other zones include the yolk transition zone (TZ) comprising the region between periplasm and yolk and the yolk (YK). Only the central ooplasm (CO) was not clear with Rhodamine B staining. CO is the egg cytoplasm that contains the yolk, which is a nutritional reserve (Fig. 1). *G mellonella* eggs post-oviposition have posterior and anterior poles (Fig. 1).

Early embryogenesis: The characteristic features of early embryonic stages were summarized in Fig. 2 and 3. Previous studies that supported visualized markers of the early morphogenesis process in lepidopteran embryonic development were identified as follows.

Table 1: Chronology of embryonic development of *Galleria mellonella* at 30±0.5°C, 85±2% RH

| Embryonic stage	Approximate age of eggs (h. PO)	State of development
1	1	Male pronucleus arrives near the egg center
	1.5-2	Fertilization
	3.5	First enegrids arrive in periplasm
2	6	Completion of cellular blastoderm
	9	Blastoderm starts to differentiate into serosa and germ disk
3	12	Formation of germ disk
	15	Serosa starts across the germ disk, which is transformed to germ rudiment
	18-22	Serosal formation
4	22-31	Germ rudiment starts to sink inside the yolk and formation of the germ band and amnion membrane during anatrepsis movement
5	31.5-40	Germ Band differentiates into PCE and PCO
6	41-60	Embryo segmentation (Appearance of Appendages in the protocephalon, Gnathal and Thoracic segments and Formation of Neural Groove)
7	61-70	Completion of elongation of Rudimentary Thoracic Appendages and Appearance of minute Pleuropodia, katatrepsis
8	71-80	Pre-Revolution. Morphogenetic movement of the cephalo-gnathal region
9	81-100	Revolution of the embryo and progress of dorsal closure
10	101-115	Completion of dorsal closure
11	116-120	Formation of primary setae and completion of dorsal closure
12	121-144	Full-grown embryo just before hatching

h: PO: Hours post-oviposition
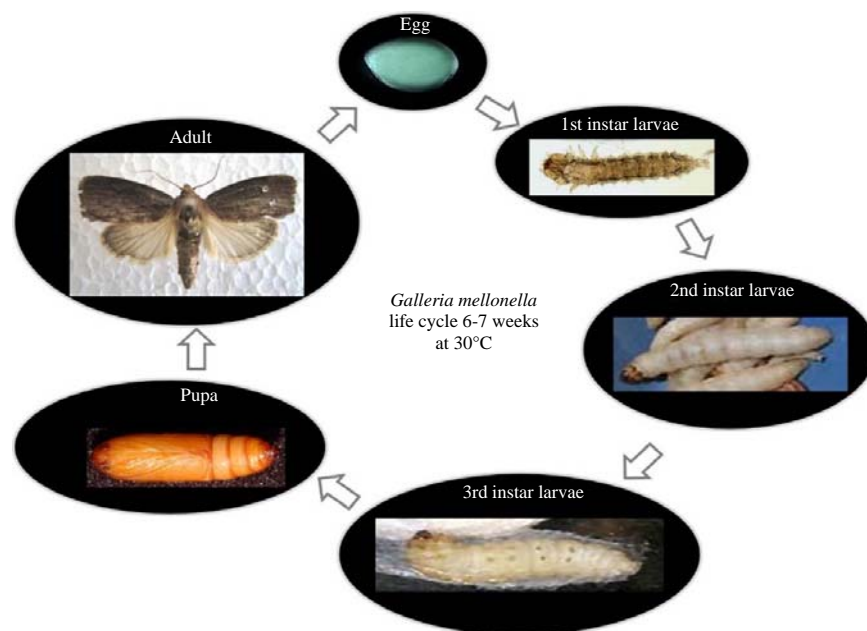
Fig. 1: Life cycle of *Galleria mellonella*. Embryogenesis stages covered
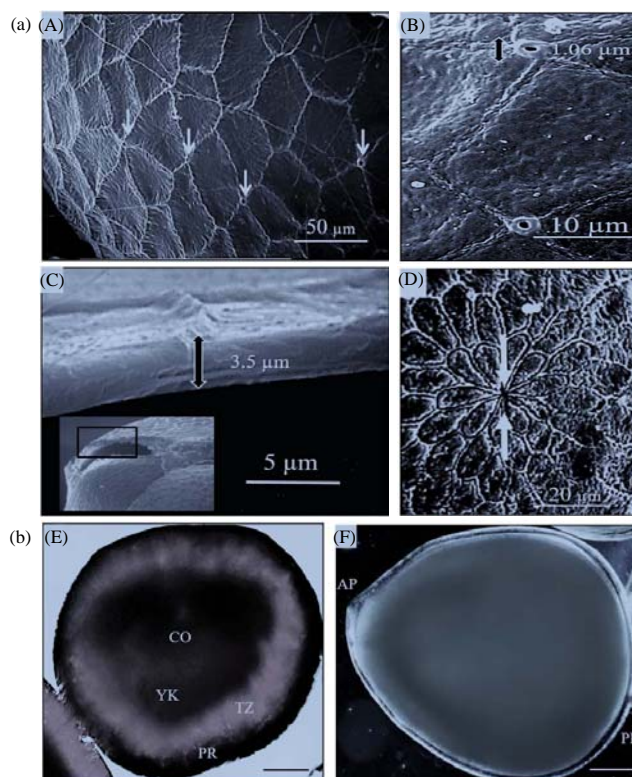

Fig. 2(a-b): (a) Morphological micrographs of the eggs of *G. mellonella*., scanning electron micrographs of external surface, A: Aeropyles (arrows), B: Aeropyle openings, with measurements, C: Chorion section showing the thickness and D: Anterior pole of the egg, showing micropyle (arrows)
(b) DIC micrographs of internal structure of the eggs after deposition, E: The egg showing the different zones of the ooplasm (PR: Periplasm, TZ: Transition zone, YK: Deutoplasm, CO: Central ooplasm) and F: Living egg just after oviposition (pp: Posterior egg pole, ap: Anterior egg pole)
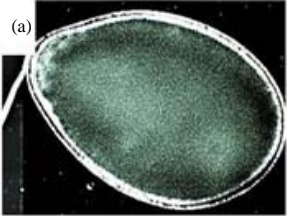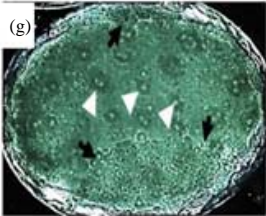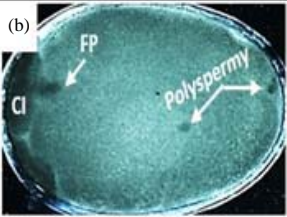A: 50 µm, B: 10 µm, C: 5 µm, D: 20 µm, E and F: 100 µm
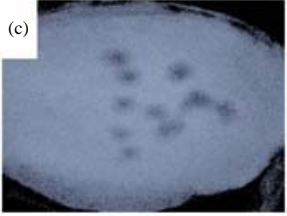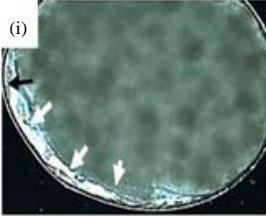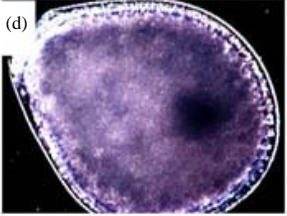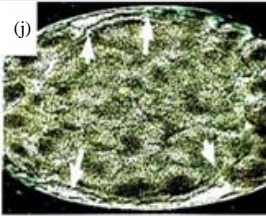
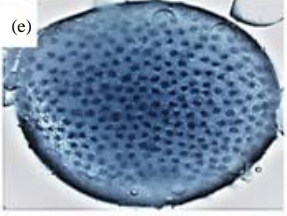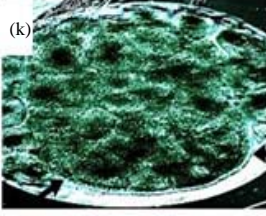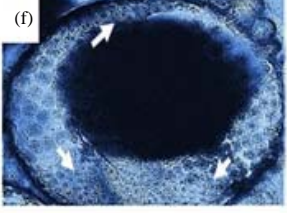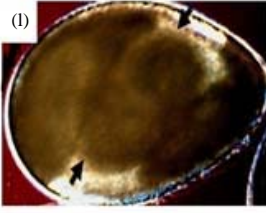| Stage (hPO)	Embryonic Characters	Embryonic development	Stage (hPO)	Embryonic Characters	Embryonic development
(1) 0-4.5	Beginning of cytoplasmic islands formation	(a)	(3) 12-22.5	Germ disk (black arrows) differentiated from primary serosa, and formation vitellophagues (white head arrows)	(g)
	Sperms pronuclei penetrates and femal pronuclei (FP) migrated to them	(b) FP CI Polyspermy		Condense and Thickening of the germ disk (white arrows)	(h)
	After fertilization anterior part and continue nuclei mitosis process	(c)		Serosa membrane (black arrows) Covering all Embryo contents (the GD (white arrows) and yolk)	(i)
(2) 5-11	Primary cellular blastoderm	(d)	(4) 22-31	Germ disk started sinks (white arrow) in yolk with formation primary amnion in dorsal edges	(j)
	Final cellular blastoderm	(e)		Germ disk (black arrows) edges surrounding the yolk cells during sinking process	(k)
(3) 12-22.5	Blastoderm (white arrows) differentiates to embryonic and extra embryonic areas	(f)		Germ disk (black arrows) sink to center of yolk with starting anatrepsis movement	(l)

Fig. 3: Overview of the development orientation in the embryos of *G. mellonella*. Scale bars of all micrographs: 100 µm

Maturation, fertilization and cleavage (0-4.5 h PO): The whole mount method is insufficient to visualize the nucleus of the female egg prior to entry of sperm that activate the female meiotic divisions. The formation phases of the cytoplasmic island (CI) in the primary post-oviposition eggs was shown in Fig. 4. A male pronucleus (MP) was clearly penetrated at completion time of CI formation. The MP was a black round spot in the yolk and its path behind it was clearly shown in the
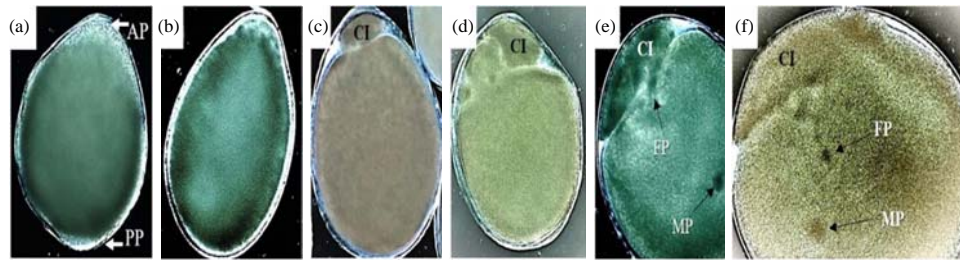
Fig. 4(a-f): DIC micrograph of the eggs of Galleria mellonella at 1st developmental stage. The development of the cytoplasmic island (CI) and its sequences is presented, (a) Egg at the beginning of CI formation, (b) The CI increases its emergence from AP side, (c) CI completion as a small ball independent from the yolk, (d) Bigger size of CI after completion shows differentiation during female mitosis divisions, (e) Kinetics of male pronucleus "MP" visualized inside the yolk and female pronucleus "FP" starts to appear as a black spot under CI and (f) FP migrates towards the MP before fertilization. Its path shows the events and the target place later

Scale bars of all micrographs: 100 μm. AP: Anterior pole, PP: Posterior pole

yolk. The CI have variable shapes and are observed near the anterior pole in the beginning of this stage. The male pronucleus migrated towards the center of the egg (fusion position) where it should meet with the female pronucleus (Fig. 3a, Fig. 4f). Female pronucleus meiosis in the CI was not visually discernible here but it is reported to occur before this migration according to observations of the same phase in other lepidopterans[35]. In three out of ten observed cases, multiple (two or three) sperm cells were visualized penetrating the egg as polyspermy (Fig. 3b). One of the male pronuclei usually fuses with the female pronucleus during syngamy, while the other pronuclei degenerate in the yolk as the CI decomposes to disappear later. Polyspermy was likewise observed in *B. mori* eggs[36] but not in other lepidopteran eggs. The progeny of the second maturation division (one female pronucleus and two polar bodies) was difficult to observe inside the CI during this stage but the division that appeared in cytoplasmic islands may be related to that mitosis (Fig. 4d). Fertilization was estimated to occur at 1.5-2 h. PO, in accordance with the second cleavage of two nuclei observed at 3 h. PO, which usually took place immediately after fertilization (Fig. 5a).

Many cleavage nuclei (energids) produced by each cleavage within a cytoplasm surrounded by a cellular membrane and the interval time (3 h) between each sample observation made it difficult to determine the exact number of energids or divisions from fertilization to the final blastoderm. Most cleavage nuclei migrated firstly toward anterior half of the periplasm (Fig. 5b), then to the posterior half of the embryo, to cover all the periplasm (Fig. 3d). At that migration time, several cleavage nuclei remained in the yolk,

where they came to resemble primary yolk nuclei or vitellophages (the nuclei arriving in the periplasm made a layer that prevented capturing the vitellophages in micrographs). The cleavage mode observed in *G. mellonella* eggs is a superficial, thus like that seen in other lepidopteran eggs. The beginning cleavage center in the anterior part of the egg was detected also in the eggs of *B. mori*[37], whereas, cleavage in the center of the egg was observed in two lepidopteran species, *M. sexta* and *D. saccharalis*[38]. Maturation, fertilization and cleavage in *G. mellonella* were generally similar to markers observed in eggs of lepidopterans such as *Endoclyta signifier* (Walker) and *E. excrescens* (Butler)[39] *B. mori*[40] and *Mnesarchaea fusilella* (Walker). The observation of early embryonic mitosis in *G. mellonella* indicates that it is analogous to that of *B. mori*.

Blastoderm formation (5-11 h PO): The cleavage nuclei, once they arrived in the periplasm, were evenly and sparsely distributed in the cytoplasm and were equidistantly separated. Gaps appeared between the future blastoderm cell borders on the anterior, posterior and dorsal surfaces of the egg (Fig. 5c). Blastoderm formation was complete at about 9 h. PO and its cells started to be found in different size and appearance according to the position inside the egg (Fig. 3d,e). In the posterior and posteroventral regions the cells were small, round and compactly arranged and each cell contained a single nucleus as well as small yolk granules. This region is the future embryonic area. In the anterior and anterodorsal regions, the blastodermal cells are large, these cells typically contained one or two nuclei and many basal yolk granules that appeared to be spatially separated from each other. This

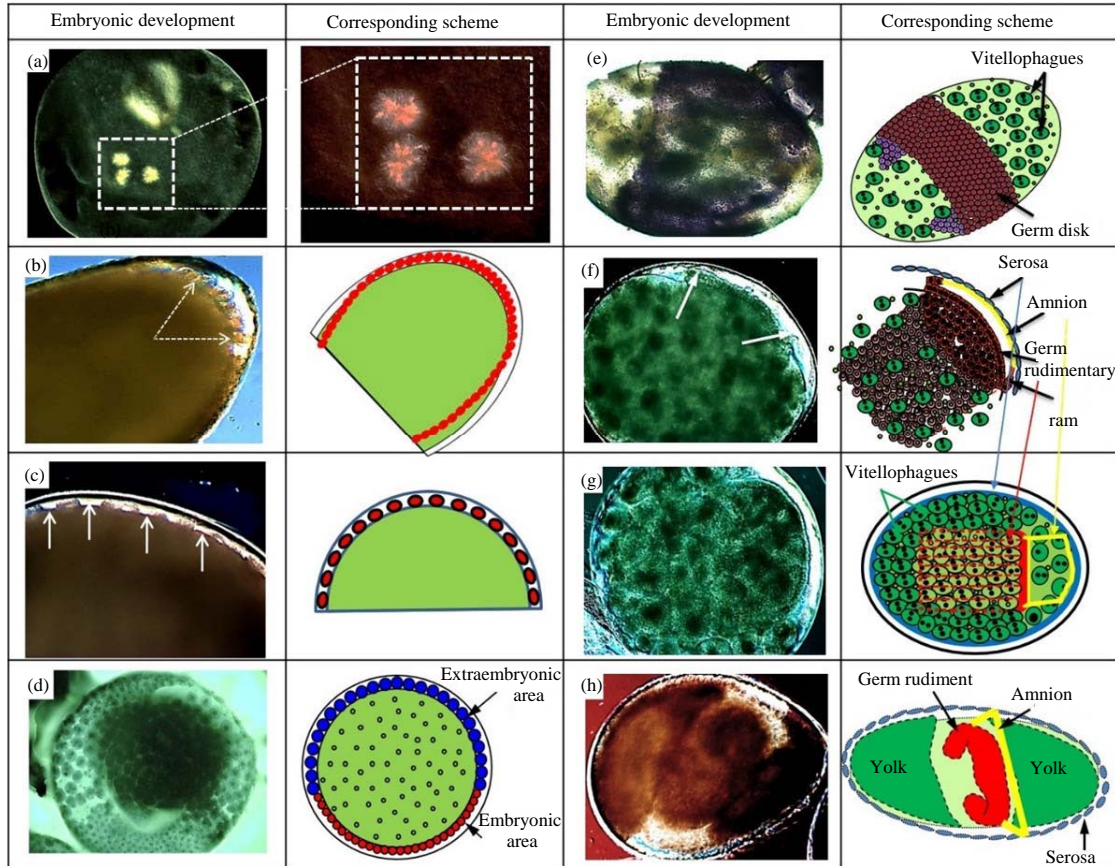| Embryonic development	Corresponding scheme	Embryonic development	Corresponding scheme

Fig. 5(a-h): Schematic representation of DIC micrographs of the sequence of early embryonic development in *G. mellonella*, (a) Second mitotic cleavage of two nuclei after fertilization, (b) The cleavage nuclei (CN) at the time of first arriving at the anterior pole, (c) The gaps (arrows) among CN that have arrived at the periplasm, (d) Blastoderm differentiated to the embryonic area and extra-embryonic area, (e) Germ disk before complete separation from serosa cells, stained with TB, (f) Germ disk (germ rudimentary GR) separated from Serosa and starting to form Amnion membrane under Serosa covering the germ rudiment, (g) GR sinks into yolk while connected to serosa membrane by the Amnion membrane and (h) GR during its movement into the yolk to transform to germ band
Scale bars of all micrographs: 100 μm

region is extra-embryonic and later will become the serosa (Fig. 5d). Blastoderm formation in *G. mellonella* eggs is different from that occurring in *B. mori* due to the lack of a uniform syncytial blastoderm[40]. The cleavage nuclei in the blastoderm become larger than the yolk nuclei as similar to *C. suppressalis* eggs. Blastulation of *G. mellonella* embryos is identical to that characterized in *B. mori*, with the same invasion of energids into the periplasm, starting anteriorly and subsequently occurring elsewhere. Conversely, in the eggs of two other lepidopteran species, *M. sexta* and *D. saccharalis*, the nucleus invasion of periplasm was synchronous due to the cleavage beginning at the egg center and all cleavage energids being equidistant from the periplasm. The blastodermal cells differ in structure between embryonic and extra-embryonic regions (Fig. 5d), this character was detected

also in other lepidopterans, including *B. mori M. sexta* and *Epiphyas postvittana* (Walker)[41]. Shape and relative size of the Germ Disk (GD) is identical to *P. rapae* and *C. suppressalis* (Ditrysia).

Germ disk, serosa formation and beginning of amnion (12-22.5 h PO): Soon after blastoderm formation, cells of the embryonic area actively proliferate to form a GD in the posterior region at about 12 h. PO (Fig. 5e, 3g). The GD is delimited from the extraembryonic area as commonly found in *P. rapae* embryos. During the formation of the GD, the amnio-serosal fold is formed along the margin of the GD (Fig. 5f, 6A, 3i). Then it shifts its position and the presumptive serosal cells flatten and fuse with another side above the separated GD to form the final serosal membrane
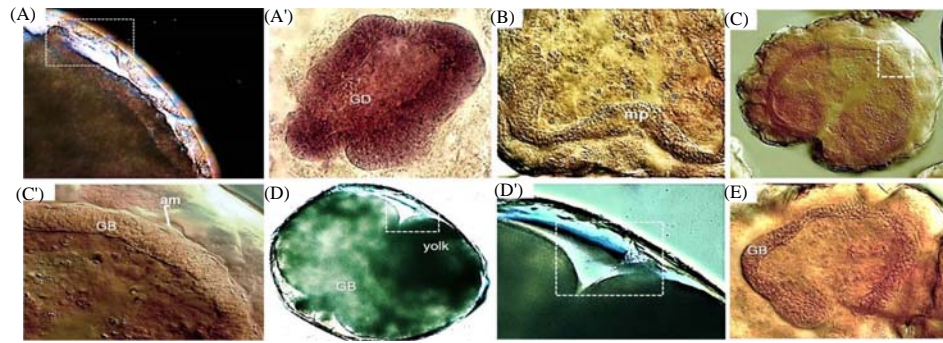
Fig. 6: DIC micrograph of the embryos of *Galleria mellonella*, A: Amnion formation starts during GD separation from serosa membrane, A': GD sinks into yolk and assumes a contrasting shape from the two pole sides during anatrepsis movement, B: Embryos similar to cross section and crescent shape show differentiation of median plate (MP), C, C': Completed amnion formation behind the extended germ band, D, D': Completed germ band surrounded the yolk showing the connection between amnion and serosa at the end of the last stage, E: The final germ band formation
Scale bars. A, E: 50 μm, B, C, D, D' and E: 100 μm

which covers the entire egg surface (Fig. 5e, f). It begins to migrate across the GD at 15 h PO. In the *G. mellonella* embryos, immediately after splitting of the GD from the serosa cells, the presumptive serosa closes above the GD and is known also as the primary serosa cuticle. This synthesizes of serosa cuticle is similar to that which occurs in *M. sexta*[42]. Because the serosal cuticle is secreted from extra-embryonic serosal cells, it is not considered an embryonic cuticle as found in the mosquito *Aedes aegypti* (Linnaeus). The GD now is large and broad and occupies more than half the surface area of the egg (Fig. 5e). The GD differentiates into a germ rudiment and the amnion and the extra-embryonic area becomes a serosal membrane. The first sign of folding is usually seen laterally along either half of the GD (Fig. 5f). The rudimentary amnion of *G. mellonella* is initially represented by a few cells around the margin of the GD, like that detected in *M. sexta*. In *G. mellonella*, the formation of two embryonic membranes (amnion and serosa) follows the fault type (F-type) which was described in monotrysian and ditrysian embryos. This type is highly specialized and rare among insects, having been observed only in lepidopterans. In that type, GD condenses toward the ventral midline, with its margin delimited from the extra-embryonic area (Fig. 5g, h). The only specific difference in the serosa formation of *G. mellonella* eggs is that the margins of the developing serosa fuse before the start of anatrepsis movement and the amnion starts before the germ disk sinks into the yolk. Similar features were also found in the eggs of other basal moths except *M. sexta*, in which the amnion starts to cover the ventral face of the GD before anatrepsis occurs[43]. It can confirm that serosa formation was completed at around 18 h PO and that the beginning of the amnion followed directly after this event.

Immersion of germ disk into the yolk, formation of the germ band during anatrepsis movement (22-31 h PO): After immersion into the yolk, the GD starts to differentiate into an amnion and germ rudiment before forming the germ band during anatrepsis movement. This movement starts post-completion of the serosa formation and sinking of the GD slightly into the yolk. The beginning of anatrepsis facilitates the amnion formation prior to the germ disk shortening in the process to form the germ band. Free margins of the GD bend toward the egg surface to grow into the narrow space between the serosa and GD, which fuse to initiate the process of forming the amnion (Fig. 5f, g, 6A). The long time needed for amnion formation may be related to the change in shape of the GD toward forming the germ band and its free movement in the yolk (Fig. 7d). The amnion continues to extend and is completed at about 32 h. PO (Fig. 6D,D'). These changes due to elongation of the germ band are distinct from anatrepsis, in that the GD initially extends in length and then shortens (Fig. 6B,E)[44], before it returns to increase in length again to become the final germ band (Fig. 6D). Connection between the serosa and the future cranial part of the embryo was observed during elongation of the germ band post-differentiation in the next stage (Fig. 6E'). Immersion of the GD into the yolk as anatrepsis movement was the first half of blastokinesis movement (Fig. 7). The extra-embryonic membrane formation in lepidopteran species differs and the difference is linked to anatrepsis movement. The GD begins its
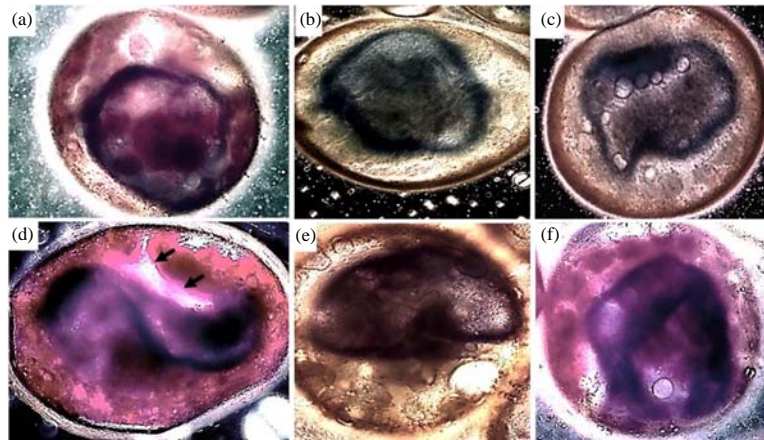
Fig. 7(a-f): DIC micrograph of the anatrepsis movement of *Galleria mellonella* embryos at 4th developmental stage (22-31 h PO), showing some parts of anatrepsis movement for formatting the germ band (24-40. PO), embryos stained with TB and Rhodamine B, (a) GD starts to sink into the center of the yolk and becomes compact from its borders, (b) GD becomes more compacted from two sides, (c) GD undergoes increased thickening and constriction at both ends, (d) Constriction of the two sides with the opposite wrap to both sides shows the white amniotic gap in ventral side of GD (black arrows) and its connection with serosa cells, (e) In this stage, the GD resembling the letter C but with shorter size and (f) Elongation and continued compression of the germ band edges (26h. PO)

Scale bars of all micrographs: 100 μm

midline shifts transitorily towards the dorsal or ventral side of the egg and begins to roll up dorsally into a flattened vesicle (Fig. 7b, c, d). The GD is passively pulled into the yolk at the posterior pole as a consequence of concentric, anteriorly directed contractions of the yolk systems. These contractions are usually associated with a cleavage of the yolk in the eggs of some species[45]. Following the cellular blastoderm formation, the embryos of most insects undergo a process of cell contraction or condensation, except for the most derived holometabolous species[46]. The contractions of the GD and its increased thickness during this process were the first step in changing its cells from cuboidal to columnar shape. The GD rotates around its anteroposterior axis, causing its ventral side to face the lateral side of the egg and to become laterally compressed (Fig. 7e). Upon reaching its maximum length, the germ band assumes a C-shape (Fig. 6E). In the final stage, two embryonic membranes, serosa and amnion, are completed. The primary serosa cuticle surrounds the yolk and germ band, while the amnion membrane covers the ventral face of the germ band and stays connected to the serosa. Anatrepsis movement and formation of the serosa and amnion membranes in *G. mellonella* were identified from resemblance to these same events in *C. suppressalis* embryos.

CONCLUSION

The process of development of the greater wax moth is similar in most parts to the type of development generally seen in Lepidoptera but with some of its own specifications. The whole mount method with short interval collection time could be an effortless way to study the embryogenesis of insect eggs that are difficult to use in sectioning preparation methods and it could reveal morphological markers that have a phylogenetic relation in same-family species. The extra-embryonic area and the formation of membranes are unknown in *G. mellonella*, it is important to understand the tissue specification, the regulation of cell shape changes and tissue interactions during morphogenesis and ascertain the functions of these membranes between morphogenetic events.

SIGNIFICANCE STATEMENT

This study is discovering the characteristics of morphogenesis of embryonic development stages in *G. mellonella* that would be beneficial for selection of proper embryonic stage that needed for cryopreservation to succeed. This study will help the researcher to uncover the critical embryonic stages and their characters to withstanding the

effects damage to the low temperature that may many researchers were not able to explore during their design for cryopreservation in Lepidopteran embryos. Thus a new theory on the importance of the early development stages for resistance the cold stress may be arrived at.

ACKNOWLEDGMENTS

REFERENCES

1.   Kristensen, N.P., 1999. Lepidoptera: Moths and Butterflies. In: Evolution, Systematics and Biogeography. Arthropoda: Insecta, Fischer, M. (Ed.), Vol. 1, Walter de Gruyter, Germany, pp: 491.

2.   Coskun, M., P. Ozalp, M. Sulanc and I. Emre, 2005. Effects of various diets on the oviposition and sex ratio of *Pimpla turionellae*. Int. J. Agric. Biol., 7: 129-132.

3.   Elawad, S.A., S.R. Gowen and N.G. Hague, 1999. The life cycle of *Steinernema abbasi* and *S. riobrave* in *Galleria mellonella*. Nematology, 1: 762-764.

4.   Glazer, I., 1997. Effects of infected insects on secondary invasion of steinernematid entomopathogenic nematodes. Parasitology, 114: 597-604.

5.   Ueno, T., 1999. Host suitability and sex-ratio differences in wild-caught and laboratory-reared parasitoid *Pimpla parnarae* (Hymenoptera: Ichneumonidae). Ann. Entomol. Soc. Am., 92: 609-614.

6.   Miyata, S., M. Casey, D.W. Frank, F.M. Ausubel and E. Drenkard, 2003. Use of the *Galleria mellonella* caterpillar as a model host to study the role of the type III secretion system in *Pseudomonas aeruginosa* pathogenesis. Infect. Immunol., 71: 2404-2413.

7.   Mylonakis, E., R. Moreno, J.B. El Khoury, A. Idnurm and J. Heitman *et al.*, 2005. *Galleria mellonella* as a model system to study *Cryptococcus neoformans* pathogenesis. Infect. Immun., 73: 3842-3850.

8.   Cymborowski, B., 1988. Effect of Cooling Stress on Endocrine Events in *Galleria mellonella*. In: Endocrinological Frontiers in Physiological Insect Ecology, Sehnal, F., A. Zabza and D.L. Denlinger (Eds.)., Technical University of Wroclaw, Poland, pp: 203-212.

9.   Cymborowski, B., 2000. Temperature-dependent regulatory mechanism of larval development of the wax moth (*Galleria mellonella*). Acta Biochim. Polonica, 47: 215-221.

10. Mikolajczyk, P. and B. Cymborowski, 1993. Lower temperature influences developmental rhythms of the wax moth *Galleria mellonella*: Putative role of ecdysteroids. Comparat. Biochem. Physiol. Part A: Physiol., 105: 57-66.

11. Roversi, P.F., E. Cosi and T. Irdani, 2008. Chill sensitivity and cryopreservation of eggs of the greater wax moth *Galleria mellonella* (Lepidoptera: Pyralidae). Cryobiology, 56: 1-7.

12. Kobayashi, Y. and G.W. Gibbs, 1995. The early embryonic-development of the mnesarchaeid moth, *Mnesarchaea-Fusilella* Walker (Lepidoptera, Mnesarchaeidae) and its phylogenetic significance. Aust. J. Zool., 43: 479-488.

13. Kobayashi, Y. and H. Ando, 1988. Phylogenetic relationships among the lepidopteran and trichopteran suborders (Insecta) from the embryological standpoint. J. Zool. Syst. Evol. Res., 26: 186-210.

14. Tanaka, M., 1981. A study on the comparative embryology of the Lepidoptera. Commemoration Number of the 90th Anniversary of Foundation, Tokyo University of Agriculture, pp: 9-21.

15. Okada, M., 1960. Embryonic development of the rice stemborer, Chilo suppressalis. Sci. Rep. Tokyo Kyoiku Daig.(Sec. B), 9: 243-296.

16. Tanaka, M., 1970. Embryonic development of the rice webworm, *Ancylomia japonica* Zeller. I. From fertilization to germ band formation. New Entomol., 19: 35-41.

17. Tanaka, M., 1972. Embryonic development of the rice webworm, *Ancylolomia japonica* Zeller. IV. From revolution to hatching. Tyo to Ga (Trans. Lep. Soc. Jap.), 23: 13-18.

18. Dossi, F.C.A., H. Conte and A.A. Zacaro, 2006. Histochemical characterization of the embryonic stages in *Diatraea saccharalis* (Lepidoptera: Crambidae). Ann. Entomol. Sci. Am., 99: 1206-1212.

19. Dorn, A., S.T. Bishoff and L.I. Gilbert, 1987. An incremental analysis of the embryonic development of the tobacco hornworm, *Manduca sexta*. Int. J. Invert. Reprod. Dev., 11: 137-157.

20. Tanigawa, N., K. Matsumoto, K. Yasuyama, H. Numata and S. Shiga, 2009. Early embryonic development and diapause stage in the band-legged ground cricket *Dianemobius nigrofasciatus*. Dev. Genes Evol., 219: 589-596.

21. Bilinski, S.M., J. Klag and J. Kubrakiewicz, 1993. Morphogenesis of accessory nuclei during final stages of oogenesis in *Cosmoconus meridionator* (Hymenoptera: Ichneumonidae). Roux's Arch. Dev. Biol., 203: 100-103.

22. Rand, M.D., A.L. Kearney, J. Daoand and T. Clason, 2010. Permeabilization of *Drosophila* embryos for introduction of small molecules. Insect Biochem. Mol. Biol., 40: 792-804.

23. Berkebile, D.R., J. Chirico and R.A. Leopold, 2000. Permeabilization of *Cochliomyia hominivorax* (Diptera: Calliphoridae) embryos. J. Med. Entomol., 37: 968-972.

24. Mazur, P., K.W. Cole and A.P. Mahowald, 1992. Critical factors affecting the permeabilization of *Drosophila* embryos by alkanes. Cryobiology, 29: 210-239.

25. Silverman, Jr., S., C. Migliorati and J. Barbosa, 1984. Toluidine blue staining in the detection of oral precancerous and malignant lesions. Oral Surg. Oral Med. Oral Pathol., 57: 379-382.

26. Rezende, G.L., A.J. Martins, C. Gentile, L.C. Farnesi, M. Pelajo-Machado, A.A. Peixoto and D. Valle, 2008. Embryonic desiccation resistance in *Aedes aegypti*: Presumptive role of the chitinized serosal cuticle. BMC Develop. Biol., Vol. 8. 10.1186/1471-213X-8-82

27. Londershausen, M., V. Kammann, M. Spindler-Barth, K.D. Spindler and H. Thomas, 1988. Chitin synthesis in insect cell lines. Insect Biochem., 18: 631-636.

28. Harrington, B.J. and G.J. Hageage, Jr., 2003. Calcofluor white: A review of its uses and applications in clinical mycology and parasitology. Lab. Med., 34: 361-367.

29. Herth, W. and E. Schnepf, 1980. The fluorochrome, calcofluor white, binds oriented to structural polysaccharide fibrils. Protoplasma, 105: 129-133.

30. Fanelli, E., M. Di Vito, J.T. Jones and C. De Giorgi, 2005. Analysis of chitin synthase function in a plant parasitic nematode, *Meloidogyne artiellia*, using RNAi. Gene, 349: 87-95.

31. Moussian, B., H. Schwarz, S. Bartoszewski and C. Nusslein Volhard, 2005. Involvement of chitin in exoskeleton morphogenesis in *Drosophila melanogaster*. J. Morphol., 264: 117-130.

32. Pavenstadt-Grupp, I. and A. Ruthmann, 1989. Microscoporidian infection in *Pimpla turionellae* (Ichneumonidae, Hymenoptera): Characteristics and reaction with Calcofluor white. Parasitol. Res., 76: 74-79.

33. Wang, W.B., R.A. Leopold, D.R. Nelson and T.P. Freeman, 2000. Cryopreservation of *Musca domestica* (Diptera: Muscidae) embryos. Cryobiology, 41: 153-166.

34. Barbier, R. and G. Chauvin, 1974. Ultrastructure et role des aeropyles et des enveloppes de l'oeuf de Galleria mellonella. J. Insect Physiol., 20: 809-820.

35. Kobayashi, Y., M. Tanaka and H. Ando, 2003. Embryology. In: Lepidoptera, moths and butterflies: Morphology, Physiology and Development, Kristensen, P.N. (Ed.). Vol. 2, Walter de Gruyter, Germany, ISBN: 978311016210, pp: 495-544.

36. Sakai, H., T. Yokoyama, H. Abe, T. Fujii and M.G. Suzuki, 2013. Appearance of differentiated cells derived from polar body nuclei in the silkworm, *Bombyx mori*. Frontiers Physiol., Vol. 4. 10.3389/fphys.2013.00235.

37. Nagy, L., L. Riddiford and K. Kiguchi, 1994. Morphogenesis in the early embryo of the lepidopteran *Bombyx mori*. Dev. Biol., 165: 137-151.

38. Takesue, S., H. Keino and K. Onitake, 1980. Blastoderm formation in the silkworm egg (*Bombyx mori* L.). Development, 60: 117-124.

39. Ando, H. and M. Tanaka, 1980. Early embryonic development of the primitive moths, *Endoclyta signifer* Walker and *E. excrescens* Butler (Lepidoptera: Hepialidae). Int. J. Insect Morphol. Embryol., 9: 67-77.

40. Kawamura, N., 1978. The early embryonic mitosis in normal and cooled eggs of the silkworm, *Bombyx mori*. J. Morphol., 158: 57-71.

41. Anderson, D.T. and E.C. Wood, 1968. The morphological basis of embryonic movements in the light brown apple moth, *Epiphyas postvittana* (Walk) (Lepidoptera: Tortricidae). Aust. J. Zool., 16: 763-793.

42. Dorn, A., 2000. Arthropoda-Insecta: Embryology. In: Reproductive Biology of Invertebrates, Adiyodi, K.G. and R.G. Adiyodi (Eds.). John Wiley and Sons, New York, pp: 71-116.

43. Kobayashi, Y. and H. Ando, 1981. The embryonic development of the primitive moth, *Neomicropteryx nipponensis* Issiki (Lepidoptera, Micropterygidae): Morphogenesis of the embryo by external observation. J. Morphol., 169: 49-59.

44. Kobayashi, Y., 1998. Embryogenesis of the fairy moth, *Nemophora albiantennella* Issiki (Lepidoptera, Adelidae), with special emphasis on its phylogenetic implications. Int. J. Insect Morphol. Embryol., 27: 157-166.

45. Panfilio, K.A., 2008. Extraembryonic development in insects and the acrobatics of blastokinesis. Dev. Biol., 313: 471-491.

46. Anderson, D.T., 1972. The Development of Holometabolous Insects. In: Developmental Systems: Insects, Counce, S.J. and C.H. Waddington (Eds.)., Academic Press, USA., pp: 165-242.